JOURNAL OF MATERIALS SCIENCE 32 (1997) 6549–6553

Characterization of a natural substituted pyromorphite

I. L. BOTTO*, V. L. BARONE, J. L. CASTIGLIONI
Química Inorgánica, CEQUINOR, Facultad de Ciencias Exactas, Universidad Nacional de La Plata, La Plata (1900), Argentina

I. B. SCHALAMUK
INREMI, Facultad de Ciencias Naturales y Museo, Universidad Nacional de La Plata, La Plata (1900), Argentina

Pyromorphite ($Pb_5(PO_4)_3Cl$) which occurs in the oxidation zone of a polymetallic Pb–Zn–Ag–Au vein in Paramillos de Uspallata, Mendoza, Argentina, was studied by scanning electron microscopy (including energy dispersive analysis of X-rays (EDAX) electron microprobe), i.r. and Raman spectroscopies and X-ray powder diffraction analysis. The substitution of Pb by Ca and Ba and Cl by OH, respectively, have been detected. In addition, i.r. absorption bands for the CO_3^{2-} ν_3-mode have been clearly identified. They are attributed to the CO_3^{2-} for PO_4^{-3} substitution in the structure. The composition is regarded as an indication of the paragenesis of the host rocks and the mineralogy of the deposit.

1. Introduction

Pyromorphite is a phosphate mineral with a nominal formula $Pb_5(PO_4)_3Cl$. It belongs to the apatite group where the fluor-apatite $Ca_5(PO_4)_3F$ is by far the commonest member. Each F ion is structurally surrounded by three Ca ions at one level. In addition, Ca–O columns are linked with PO_4^{-3} groups forming a hexagonal network [1–4].

The structural characteristic is that it allows extensive and varied substitutions in all positions of the structure. The incorporation of elements belonging to groups I, II and III as well as Pb, Cd, Zn, Sc, Y, Cr, Fe, REE, Bi, U, etc., occurs at the Ca position in fluor-apatite structure [5], while the PO_4^{3-} group can be substituted by SiO_4^{4-}, SO_4^{2-}, VO_4^{3-}, CO_3^{2-}, AsO_4^{3-}, CrO_4^{2-}, etc [6]. HPO_4^{2-} and possibly $H_2PO_4^{-}$ can be incorporated in the PO_4 sites to compensate the deficiencies of the Ca sites [7]. Besides, fluorine, chlorine, hydroxyl, oxide and carbonate ions can mutually replace each other [8].

Apatite is a common accesory mineral in many types of rocks and in most abundant phosphorus-bearing minerals [4]. All possible replacements in natural apatites are influenced by the environment in which the mineral forms. Certain members of the apatite group present appreciable quantities of CO_2 (as much as 5 or 6%) [4]. Studies on the genesis of the carbonate apatites show that their formation depends on the presence of alkaline phosphate solutions and is a function of the pH and the PO_4^{3-}/HCO_3^{-} content in the solution [4].

Substitutions produce variations in the apatite hexagonal unit cell parameters and particularly in the chemical properties of these materials [9].

Pyromorphite is a lead apatite where the Ca and F of the typical apatite are replaced by Pb and Cl, respectively. The hexagonal cell parameters for pure $Pb_5Cl(PO_4)_3$ are $a = 0.9987$ nm $c = 0.733$ nm, with space group = $P6_3/m$ (PDF 19-701).

It is interesting to remark that the term "pseudoapatite" is mostly used in literature for calcium phosphates pseudomorphic to pyromorphite [10]. In this context, crystals of halogenapatite can be formed directly by replacement of existing pyromorphite or grow epitactically on the primary mineral.

Because apatites are common accessory minerals in rocks of almost all origins (igneous, metamorphic, sedimentary) and owing to the great number of substitutions in this type of structure, they are good indicators of the genetic conditions of the host rocks [11].

The purpose of this paper is to study the chemical and structural characterization of a natural pyromorphite from the oxidation zone of a polymetallic vein of Paramillos de Uspallata mineral district [12] and to reveal the interaction of the mineral with the mineralizing components and the host rock in the deposit. The study has been carried out by means of X-ray powder diffraction analysis (XRPD) and scanning electron microscopy (SEM) including energy dispersive analysis of X-rays (EDAX) electron microprobe. The vibrational spectrum has been also analysed in detail in relation to the chemical composition of the

* Author to whom correspondence should be addressed.

0022–2461

samples, and it has indicated the presence of different substitutions in the structure through their effects on the fundamental vibrations. The results are compared with those of other reported lead phosphates.

2. Experimental procedure

Pyromorphite samples were obtained from Paramillos de Uspallata, mineral district, Mendoza, Argentina [12].

The main primary mineralization of this zone is galena, pyrite, sphalerite, chalcopyrite, marcasite, arsenopyrite, bornite, tetrahedrite, proustite and argentite. Jordanite and gratonite are minor constituents. The sulphosalt minerals are associated with the carbonates siderite, calcite, rhodocrosite and a small proportion of barite. Limonite and Mn-oxides (as alteration products of Mn- and Fe- carbonates), malachite, azurite, cerargyrite, iodo- and bromoargyrite, and cerussite are the main components of the oxidation zone where the pyromorphite has been found.

Single crystals of pyromorphite were carefully selected by hand. Samples were washed with acetone and dried at 120 °C. The purity of the samples was checked by X-ray diffraction analysis with a Philips PW 1714 diffractometer (CuK_α radiation, Ni filtered). The data was collected using Si as external standard. Cell parameters were refined by means of the Werner version of PIRUM program [13].

The i.r. spectra were recorded in a Perkin Elmer 580-B spectrophotometer using the KBr pellet technique. Raman spectra were registered in a Bruker IFS-66 spectrometer equipped with a Nd–YAG laser.

Samples were also analysed by SEM scanning electron microscopy in a Philips 505 electron microscope with an EDAX 9100 microprobe with an energy dispersive detector. The values of microprobe analysis were the average of several points in each sample. No significant differences among the measurements have been appreciated. The thermal analysis was carried out in a Pt-crucible at a muffle furnace up to 1000 °C.

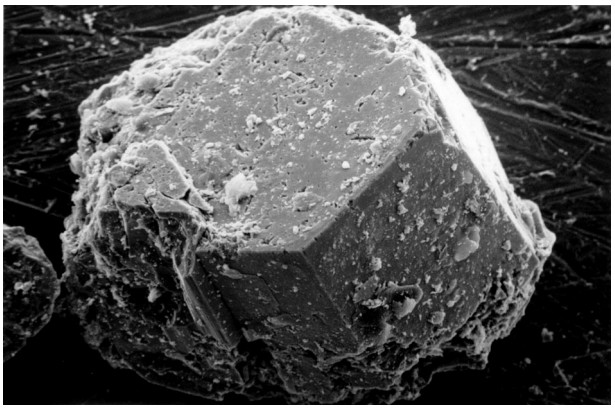

Figure 1 Micrograph of pyromorphite specimen from Paramillos de Uspallata, Mendoza, Argentina (magnification × 500; scale bar 100 μm).

TABLE I Comparison of cell dimensions of some apatite phases

Compound	a (nm)	c (nm)	Ref.
Pyromorphite from Paramillos de Uspallata	1.002 (1)	0.737 (1)	This work
Pyromorphite natural	1.0	0.733	PDF 12-704
$Pb_5(PO_4)_3Cl$ synthetic	0.9987	0.733	PDF 19-701
$Pb_5(PO_4)_3(OH)$	0.9987	0.7427	PDF 8-259
$Ca_{0.52}Pb_{4.48}(PO_4)_3(OH)$	0.983	0.737	[a]
$Ca_{4.51}Pb_{0.49}(PO_4)_3(OH)$	0.946	0.691	[a]
$Ca_5(PO_4)_3(OH)$	0.9418	0.6884	PDF 9-432
$Ca_5(PO_4)_3Cl$	0.9641	0.6771	PDF 33-271
$Ba_5(PO_4)_3(OH)$	1.019	0.77	[b]
$Ca_{10}(PO_4)_5CO_3F_{1.5}(OH)_{0.5}$ natural sample	0.9346	0.6887	PDF 31-267
$Ca_5(PO_4)_3F$	0.9368	0.688	PDF 15-876
Carbonate-apatite (francolite type) (CO_3^{2-} for PO_4^{3-})	0.936	0.689	[c]
Carbonate-apatite (CO_3^{2-} for OH)	0.955	0.687	[c]

[a] M. Andres-Verges, F. J. Highes-Rolando, C. Valenzuela-Calahorro and P. F. Gonzalez Diaz, *Spectrochim. Acta* **39A** (1983) 1077.
[b] K. C. Blakeslee and R. A. Condrate, *J. Amer. Ceram. Soc.* **54** (1971) 559.
[c] G. Bonel, *Ann. Chim.* **127** (1972) 144.

3. Results and discussion

The typical morphology of hexagonal apatite crystals has been found for the pyromorphite crystals, as shown in Fig. 1 [10, 14]. The microprobe chemical analysis yields the following average values (as weight % of the EDAX registered elements): P = 8.00, Cl = 1.44, Pb = 88.75, Ca = 0.17, Ba = 1.64, with a P/divalents = 8.83×10^{-2} lower than that observed for pure pyromorphite (theoretical values: P = 7.98, Cl = 3.04, Pb = 88.97, P/divalent = 8.97×10^{-2}). The Cl/divalent ratio is also lower for the analysed sample (1.59×10^{-2} versus 3.41×10^{-2} for pure pyromorphite), whereas the opposite is observed for the P/Cl ratio (5.55 and 2.62, respectively). These data suggest the substitution of PO_4 and Cl by CO_3 and OH, respectively (not detected by EDAX). However, the weight-loss at 1000 °C, ($\sim$ 1.1%), corroborates the presence of volatiles as H_2O and CO_2 from the structure.

The XRPD analysis reveals the typical lines of pyromorphite (PDF 19-701). The refined *a* and *c* cell parameters are given in Table I, where the crystallographic data of other members of the apatite family are included for comparison. A very slight difference between our experimental data and those reported for synthetic pyromorphite is caused by the substitutions. No significant effect is expected in the cell dimensions of the substituted pyromorphite when Pb is replaced by Ca and Ba simultaneously, according to their respective ionic radii ($r_{Ca(II)} = 0.118$ nm, $r_{Ba(II)} = 0.147$ nm, $r_{Pb(II)} = 0.135$ nm [15]. It was established that the cell dimensions of CO_3^{2-}–PO_4^{3-} substituted apatites only show appreciable differences for higher CO_3^{2-} contents [16].

Fig. 2 shows the vibrational spectrum of the studied specimen. It is well known that isolated PO_4 tetrahedral ions present T_d symmetry with four normal modes

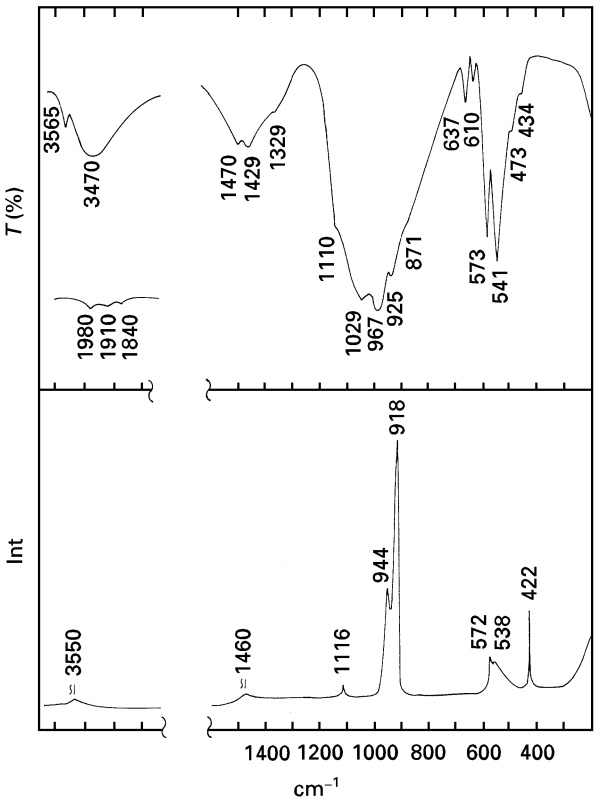

Figure 2 Vibrational spectrum of pyromorphite (top, i.r; bottom, Raman).

of vibration: ν_3 and ν_1 antisymmetric and symmetric P–O stretchings (at 1017 and 938 cm^{-1}, respectively) and ν_2 and ν_4 antisymmetric and symmetric O–P–O bending modes (at 420 and 567 cm^{-1}) [17]. The four vibrations are all Raman active whereas only ν_3 and ν_4 are i.r. active. The PO_4 site symmetry in the pure pyromorphite lattice is lowered to C_S [18]. The correlation among the tetrahedral free ion, the site group model (C_s) and the factor group analysis (C_{2h}) is shown in Table II. So, the nine internal modes are expected to be highly split in the crystal. However, the number of bands predicted by factor group analysis is not observed. This can be explained by the shielding effect of the Pb atoms which led to an interaction among tetrahedral groups which was lower than in the calcium apatite [19]. Likewise, the position of the PO_4 bands does not show important deviation from pure pyromorphite [19–23].

Although the Raman spectrum does not show a very good resolution (in particular the PO_4 bending lines), its most intense lines can be attributed to the ν_3 and ν_1 P–O stretching modes which are located at 944 and 918 cm^{-1}, respectively. The equivalent i.r. bands are located at 1029, 967 cm^{-1} (ν_3) and 925 cm^{-1} (ν_1). These values are slightly higher than those observed for pure pyromorphite [18]. However, it is evident that the strongest i.r. band is asymmetric, with shoulders at 1110 and 871 cm^{-1}. This feature, as well as the weak bands at 1468, 1429 and 1329 cm^{-1} can be attributed to the CO_3^{2-} specie. This free ion, with D_{3h} planar symmetry also shows four normal modes of vibration. The symmetry can be, however, lowered

TABLE II Correlation among the symmetry of the PO_4^{3-} "free ion", the site symmetry C_S and the factor group analysis C_{2h}

"Free ion" T_d	Site symmetry C_S	Factor group C_{2h}
ν_1 (A_1)	A'	$A_g + E_{2g} + B_u + E_{1u}$
ν_2 (E)	$A' + A''$	$A_g + E_{2g} + B_u + E_{1u}$
		$B_g + E_{1g} + A_u + E_{2u}$
ν_3 (F_2)	$2A' + A''$	$2A_g + 2E_g + 2B_u + 2E_{1u}$
		$B_g + E_{1g} + A_u + E_{2u}$
ν_4 (F_2)	$2A' + A''$	$2A_g + 2E_g + 2B_u + 2E_{1u}$
		$B_g + E_{1g} + A_u + E_{2u}$
i.r. activity: F_2	A' and A''	A_g, E_{2g} and E_{1g}
Raman activity:	A' and A''	E_{1u} and A_u
A_1, E and F_2	A' and A''	
Inactive: –	–	B_u, B_g and E_{2u}

ν_1 (A_1) symmetric stretching.
ν_2 (E) symmetric bending.
ν_3 (F_2) antisymmetric stretching.
ν_4 (F_2) antisymmetric bending.

in the crystalline state with the subsequent activation and splitting of the modes. The i.r.-ν_1 symmetric stretching mode is located at ~1150 cm^{-1} whereas the ν_3 antisymmetric components appear in the 1400–1500 cm^{-1} region. The bending vibrations are located at ~700 and ~860 cm^{-1} regions [17]. The number and characteristics of the ν_3 components undoubtedly indicate the place where the CO_3 ion is located in the apatite structure [9, 24]. So, the absence of i.r. bands above 1500 cm^{-1} and the shifting of the bending modes to lower wavenumbers confirm the replacement at the PO_4 site only. The relative sharpness of the phosphate Raman vibrations reasserts this assumption, and corroborates that the incorporation of carbonate is small [25].

Carbonate-apatites of francolite or dahllite type (PO_4^{3-} replaced by CO_3^{2-}) are slightly defective concerning the respective divalent ion content in relation to the ideal formula [25]. In the particular case of apatites with vacancies, i.r. spectroscopy can provide not only the CO_3 site, but also a better representation of the unit cell symmetry than X-ray diffraction. The perturbations of the phosphate vibrations may be explained as the results of differences in the crystalline field around the tetrahedral group, according to the distances from the divalent ion and the vacancy, respectively.

In order to clarify the assignment of the i.r. spectrum in the region between 700 and 1200 cm^{-1} the enveloping curve is decomposed into the number of the Lorentzian components expected for all the anionic species in the lattice. The fitting is accomplished by means of a last square procedure, and the results are plotted in Fig. 3. Four of the Lorentzian components are associated to the PO_4 group (three ν_3 antisymmetric P–O components at 1073, 1033 and 968 cm^{-1} and the fourth one to the ν_1 symmetric mode at 913 cm^{-1}), while the bands related to the CO_3 at the PO_4 site are ν_1 at ~1119 cm^{-1} and ν_2 at 861 cm^{-1}. The other two bands at 803 and 748 cm^{-1} could be associated with the librations of the strongest OH bonds as mentioned below.

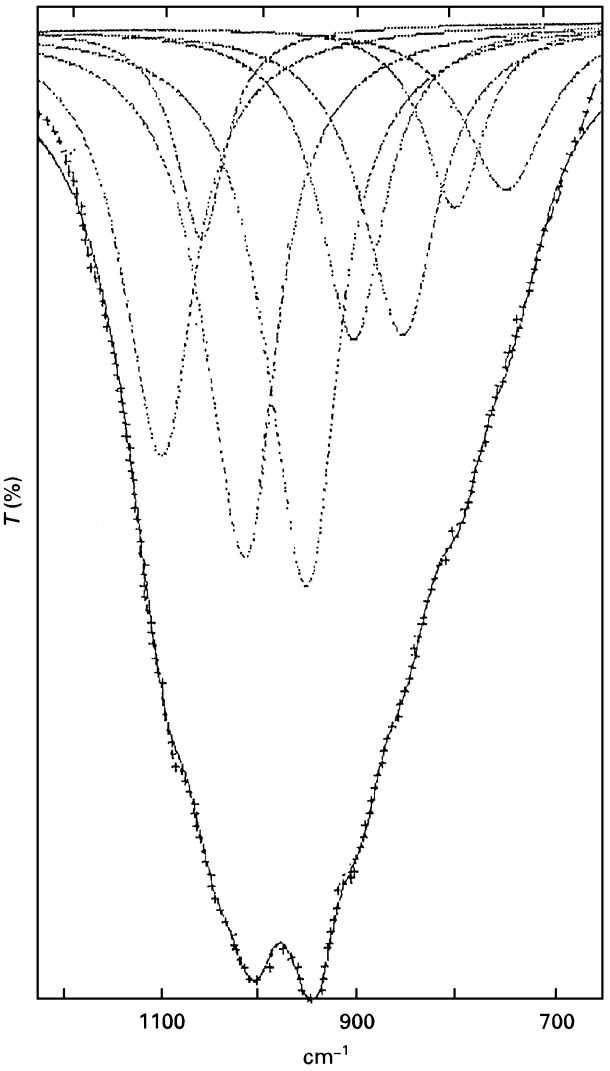

Figure 3 The observed (----) and the fitted (xxxx) i.r. spectrum in the 1000 cm^{-1} region (including the Lorentzian components).

On the other hand, the strong i.r. bands at 573 and 541 cm^{-1} are attributed to the ν_4 mode of the PO_4 group, in agreement with the assignment given for $Pb_5(PO_4)_3Cl$ and $Pb_5(PO_4)_3(OH)$ [18]. The corresponding Raman modes appear as weak lines at 572 and 538 cm^{-1}, respectively. Finally, the weak i.r. and Raman signals between 400 and 480 cm^{-1} (473 sh, 434 sh, in IR spectrum and 422 in the Raman effect) are associated with the ν_2 vibration of the tetrahedral group [17].

The series of very weak i.r. bands between 1850 and 2000 cm^{-1} (approximately at 1980, 1910 and 1840 cm^{-1}), also observed in the i.r. spectra of calcium, strontium and barium hydroxyapatites, correspond to overtones and combinations ($2\nu_3$, $\nu_3 + \nu_1$, $2\nu_1$) [26]. Obviously, they occur at lower wavenumbers than those of Ca- and Sr-apatites, concomitant with the lower wavenumber of the main bands for the pyromorphite.

In i.r. spectra, the characteristic OH vibrations are represented by the wavenumbers and intensities of OH stretching mode (3530–3570 cm^{-1}) and the librational and translatory modes (650–750 cm^{-1} and ~350 cm^{-1}, respectively). The Raman lines are, however, very weak and diffuse.

As the OH content in the apatite phase increases, so does the intensity of the i.r. modes. Likewise, the librational modes are shifted to lower wavenumbers [26]. The feature of the highest bands (a sharp band at 3563 cm^{-1} and the broad band centred at 3470 cm^{-1}) suggests the presence of two types of H bonding: from the nearest oxygen atoms of the PO_4 units and from the OH and Cl ions of the channels. The broad band indicates a H bond of moderate strength. The assumption of a disordered distribution of the OH and Cl ions and a local reinforcement of some hydroxyl groups is supported by the presence of the band at a higher wavenumber [27]. It has been established that the structural interaction between chlorine and the hydroxyl groups into the apatite lattice leads to a OH … Cl hydrogen bond which is stronger than the bond in OH … F apatite. This abnormal behaviour, based on geometrical site requirements, leads to a contraction of the *a* axis [28, 29].

In addition, the shoulder at 1100 cm^{-1} could be also related to the incorporation of the OH group. In fact, a band at 1130 cm^{-1} has been observed in chlorohydroxyapatite, whereas it is absent in the chloroapatite spectrum. This has been attributed to a lowering of the unit cell symmetry, although the change is undiscernible by XRPD. This new contribution to a change of the crystalline field around the phosphate group may be due to the closeness of this group to both monovalent anions. Likewise, the weak bands at 610 and 637 cm^{-1} attributable to hydroxyl librations confirm the presence of a hydrogen bonding of moderate strength. In fact, when this bond is of moderate strength, the hindered motion of the OH groups is more restricted. This produces an increase in the wavenumber values as well as the appearance of additional bands of diffuse intensity at higher frequencies (~755 and ~795 cm^{-1} in chlorohydroxyapatites [29]). Because of these bands it was very difficult to obtain the fit of Fig. 3, especially at the beginning when only the contribution of the PO_4 and CO_3 species was considered. But it is clear that the complex vibrational behaviour of the OH groups depends on several factors, and particularly on local structural changes [30].

As Cl and OH are the only species located in the channels on the six-fold axis, and on the basis that the Cl content is a datum from microprobe analysis, the Cl/OH monovalent ratio can be established as ~1. Likewise, from the weight loss produced by heating at 1000 °C, a CO_3 content of ~0.8% can be also estimated. These data contribute to the estimation of the formula for the substituted pyromorphite as follows

$$(Pb_{1-m-n}\,Ca_m\,Ba_n)_{10-x+u}(PO_4)_{6-x}(CO_3)_x \times [Cl_{1-z}(OH)_z]_{2-x+u}$$

where $m \sim 0.01$, $n \sim 0.027$, $x \sim 0.3$, $u \sim x/2$, $z \sim 0.45$.

The complete assignment of the vibrational spectrum of the substituted pyromorphite from Paramillos de Uspallata, Argentina is given in Table III.

Finally, the genesis of pyromorphite in this mineral district might be interpreted as the oxidation product of the primary lead mineral (galena) which has been

TABLE III Assignment of the substituted-pyromorphite vibrational spectrum (in cm^{-1})

i.r.	Raman	Assignment
3565 w	3550 vw (broad)	ν O–H
3470 w (broad)		
1980 vw		Overtones and
1910 vw		combinations
1840 vw		of ν P–O
1470 w	1460 vw	
1429 w		$\nu_3\ CO_3^{2-}$
1329 sh		
1110 sh	1116 vw	$\nu_1\ CO_3^{2-}$
1029 vs		$\nu_3\ PO_4^{3-}$
967 vs	944 m	
925 sh	918 vs	$\nu_1\ PO_4^{3-}$
871 sh		$\nu_2\ CO_3^{2-}$
637 w		Lib. OH
610 w		
573 s	572 w	
541 s	538 w (broad)	$\nu_4\ PO_4^{3-}$
473 sh		$\nu_2\ PO_4^{3-}$
434 sh	422 m	

vs: very strong, s: strong, m: medium, w: weak, vw: very weak, sh: shoulder.

affected by phosphate-rich fluids in an environment of alkaline carbonates. The morphology and size of the crystals suggest a slow growing process to form high quality single specimens.

4. Conclusions

The present study supports the following information:

1. The formation of a substituted pyromorphite has been proved. The mineral shows the following approximate formula

$$(Pb_{0.963}Ca_{0.01}Ba_{0.027})_{9.85}(PO_4)_{5.7}(CO_3)_{0.3} \times [Cl_{0.90}(OH)_{1.1}]$$

2. The cell parameters are practically unaffected by the ionic replacements because of opposite size effects of the substituting divalent ions. The slight variation may be mostly related to the Cl–OH substitution.

3. From the spectroscopic point of view, it is possible to affirm that:

(a) the CO_3 ion is incorporated in the PO_4 site of the structure.

(b) the incorporation of a small proportion of CO_3 and other substituents (Ba, Ca and OH) has little or no effect on the strength of the P–O bonds.

(c) the incorporation of OH in the structure produces a moderate H bond which is originated by the interactions between the OH groups with the oxoanions and the other monovalent anions in the structure. A disordered distribution of these ions in the channels is also suggested.

4. The incorporation of Ba, Ca and CO_3 in the structure can be supported by the mineralogical paragenesis of the ore deposit.

Acknowledgements

This work was supported by CONICET and CICPBA. The authors wish to thank Lic. M. A. Sanchez (CINDECA) for technical assistance.

References

1. J. C. ELLIOT, *Science* **230** (1971) 72.
2. A. BAUMER, M. GANTEAUME and W. E. KLEE, *Bull. Miner.* **108** (1985) 145.
3. J. C. ELLIOT, P. E. MACKIE and R. A. YOUNG, *Science* **180** (1973) 1055.
4. W. A. DEER, R. A. HOWIE and J. ZUSSMAN, "Rock forming minerals" 5 (Green & Co. Ltd., London, 1962) p. 324.
5. D. McCONNELL, *Amer. Mineral.* **23** (1938) 1.
6. E. E. BERRY, *J. Inorg. Nucl. Chem.* **29** (1967) 317.
7. W. P. ROTHWELL, J. S. WAUGH and J. P. YESINOWSKI, *J. Amer. Ceram. Soc.* **102** (1980) 2637.
8. Y. LIU and P. COMODI, *Mineral. Mag.* **57** (1993) 709.
9. G. BONEL, *Ann. Chim.* **7** (1972) 65, 127.
10. L. NASDALA, *N. Jahr. Miner. Abh.* **164** (1992) 211.
11. W. P. NASH, "Phosphate minerals", edited by J. O. Nriagu and P. B. Moore (Springer Verlag, New York, 1984) p. 275.
12. M. GARRIDO, I. B. SCHALAMUK and E. DOMINGUEZ, *Actas Mineral. Metal. La Plata* (*Argentina*) **2** (1994) 131.
13. P. E. WERNER, *Ark. Kemi.* **31** (1969) 513.
14. V. ANGELELLI, M. BRODTKORB, C. GORDILLO and H. D. GRAY, "Las especies minerales de la República Argentina", (Servicio Minero Nac., Argentina, 1983).
15. R. D. SHANNON, *Acta Crystallogr.* **A32** (1976) 751.
16. R. ZAPANTA LeGEROS, *Nature* **206** (1965) 403.
17. K. NAKAMOTO, "Infrared and Raman spectra of inorganic and coordination compounds" (John Wiley & Sons, New York, 1986).
18. W. E. KLEE and G. ENGEL, *J. Inorg. Nucl. Chem.* **32** (1970) 1837.
19. S. R. LEVITT and R. A. CONDRATE, *Amer. Mineral.* **55** (1970) 1562.
20. M. ANDRES VERGES, F. J. HIGES ROLANDO, C. VALENZUELA CALAHORRO and P. F. GONZALEZ DIAZ, *Spectrochim. Acta* **39A** (1983) 1077.
21. P. F. GONZALEZ DIAZ and M. SANTOS, *ibid.* **34A** (1978) 241.
22. V. C. FARMER, "The IR spectra of minerals", (Minerals Society, London, 1974).
23. A. BIGI, M. GANDOLFI, M. GAZZANO, A. RIPAMONTI, N. ROBERI and S. A. THOMAS, *J. Chem. Soc. Dalton Trans.* (1991) 2883.
24. M. SANTOS and P. F. GONZALEZ DIAZ, *Inorg. Chem.* **16** (1977) 2131.
25. D. G. A. NELSON and B. E. WILLIAMSON, *Aust. J. Chem.* **35** (1982) 715.
26. B. O. FOWLER, *Inorg. Chem.* **13** (1974) 194.
27. R. A. YOUNG, W. VAN der LUGT and J. C. ELLIOT, *Nature* **223** (1969) 729.
28. G. C. MAITI and F. FREUND, *J. Inorg. Nucl. Chem.* **43** (1981) 2633.
29. K. SUDARSANAN and R. A. YOUNG, *Acta Crystallogr.* **B34** (1978) 1401.
30. S. B. ETCHEVERRY, M. C. APELLA and E. J. BARAN, *J. Inorg. Biochem.* **20** (1984) 289.

Received 17 June 1996
and accepted 9 May 1997